



Supplement of

Global flood exposure from different sized rivers

Mark V. Bernhofen et al.

Correspondence to: Mark V. Bernhofen (cn13mvp@leeds.ac.uk)

The copyright of individual parts of the supplement might differ from the article licence.

Contents

S1 Model Calibration	1
S2 Model Validation	6
S2.1 Validation Against Existing Models	6
S2.2 Validation Against Observed Events	19
S3 Top 50 Countries Exposure	21
S4 HRSL Missing Countries	23
S5 GFM Coverage Maps	24
S6 References	27

S1 Model Calibration

The globe was split into five simplified climate zones (*Figure S1*). The 30 Köppen-Geiger climate classifications (Beck et al., 2018) were categorized into five climate zones as follows: **Tropical** (Af – Tropical, rainforest; Am – Tropical, monsoon; Aw – Tropical, savannah), **Arid** (BWh – Arid, desert, hot; BWk – Arid, desert, cold; BSh – Arid, steppe, hot;

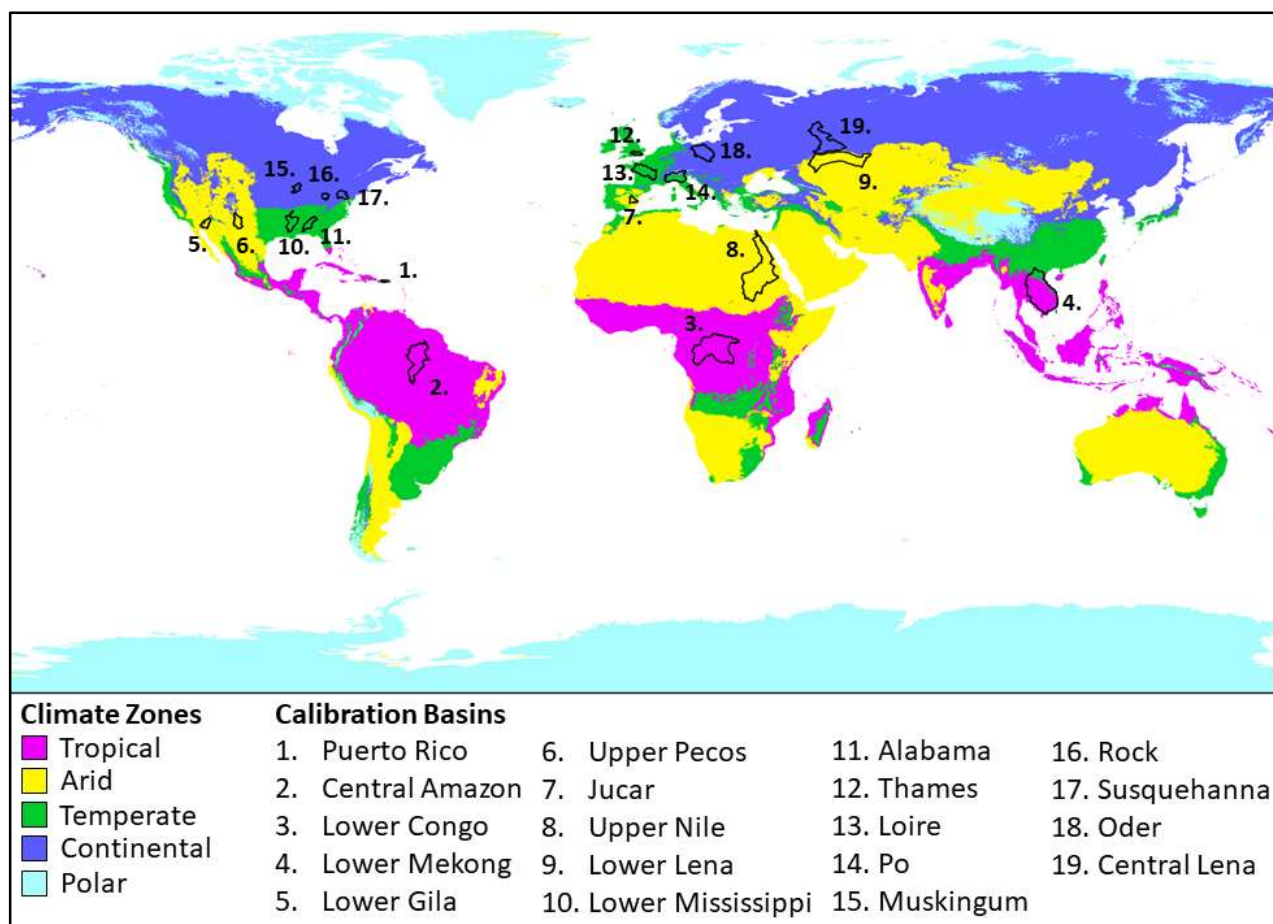


Figure S1. Map of Model Calibration Basins and Simplified Köppen-Geiger Climate Classifications

BSk – Arid, steppe, cold), **Temperate** (Csa – Temperate, dry summer, hot summer; Csb – Temperate, dry summer, warm summer; Csc – Temperate, dry summer, cold summer; Cwa – Temperate, dry winter, hot summer; Cwb – Temperate, dry winter, warm summer; Cwc – Temperate, dry winter, cold summer; Cfa – Temperate, no dry season, hot summer; Cfb – Temperate, no dry season, warm summer; Cfc – Temperate, no dry season, cold summer),

Continental (Dsa – Cold, dry summer, hot summer; Dsb – Cold, dry summer, warm summer; Dsc – Cold, dry summer, cold summer; Dsd – Cold, dry summer, very cold winter; Dwa – Cold, dry winter, hot summer; Dwb – Cold, dry winter, warm summer; Dwc – Cold, dry winter, cold summer; Dwd – Cold, dry winter, very cold winter; Dfa – Cold, no dry season, hot summer; Dfb – Cold, no dry season, warm summer; Dfc – Cold, no dry season, cold summer; Dfd – Cold, no dry season, very cold winter), **Polar** (ET – Polar, tundra; EF – Polar, frost).

Our River Flood Susceptibility Model (RFSM) was calibrated against reference flood maps in 19 different calibration basins globally. These calibration basins, visualized in *Figure S1*, span all climate zones (except Polar regions). The aim in choosing the calibration basins was to ensure that for each climate zone we had reference flood maps for rivers of all Strahler stream orders. We use 4 different reference flood maps: FEMA’s 100 year national flood hazard layer (<https://www.fema.gov/flood-maps/tools-resources/flood-map-products/national-flood-hazard-layer>), The Environment Agency’s 100 year flood map for planning (<http://apps.environment-agency.gov.uk/wiyby/cy/151263.aspx>), JRC’s 100 year flood map for Europe (Dottori et al., 2016b), and JRC’s Global 100 year flood map (Dottori et al., 2016a). The 100-year return period was chosen as it was the only return period consistent across all the datasets. *Table S1* summarizes each of the calibration basins and the reference flood map used. *Figure S2* shows maps of each of the calibration basins and visualizes the reference flood maps within the basins.

Table S1. Calibration Basin Information

#	Basin Name	Climate Zone	Reference Flood Map	Strahler Orders
1	Puerto Rico	Tropical	FEMA 100 YR	1-5
2	Central Amazon	Tropical	JRC GLOBAL 100 YR	6-8, 11
3	Lower Congo	Tropical	JRC GLOBAL 100 YR	5-10
4	Lower Mekong	Tropical	JRC GLOBAL 100 YR	6-10
5	Lower Gila	Arid	FEMA 100 YR	1-6, 9-10
6	Upper Pecos	Arid	FEMA 100 YR	1-7
7	Jucar	Arid	JRC EU 100 YR	4-7
8	Upper Nile	Arid	JRC GLOBAL 100 YR	6-10
9	Lower Lena	Arid	JRC GLOBAL 100 YR	6-9, 11
10	Lower Mississippi	Temperate	FEMA 100 YR	1-10
11	Alabama	Temperate	FEMA 100 YR	1-7
12	Thames	Temperate	EA 100 YR	1-6
13	Loire	Temperate	JRC EU 100 YR	4-9
14	Po	Temperate	JRC EU 100 YR	4-8
15	Muskingum	Continental	FEMA 100 YR	1-7
16	Rock	Continental	FEMA 100 YR	1-7
17	Susquehanna	Continental	FEMA 100 YR	1-8
18	Oder	Continental	JRC EU 100 YR	4-9
19	Central Lena	Continental	JRC GLOBAL 100 YR	6-7, 10-11

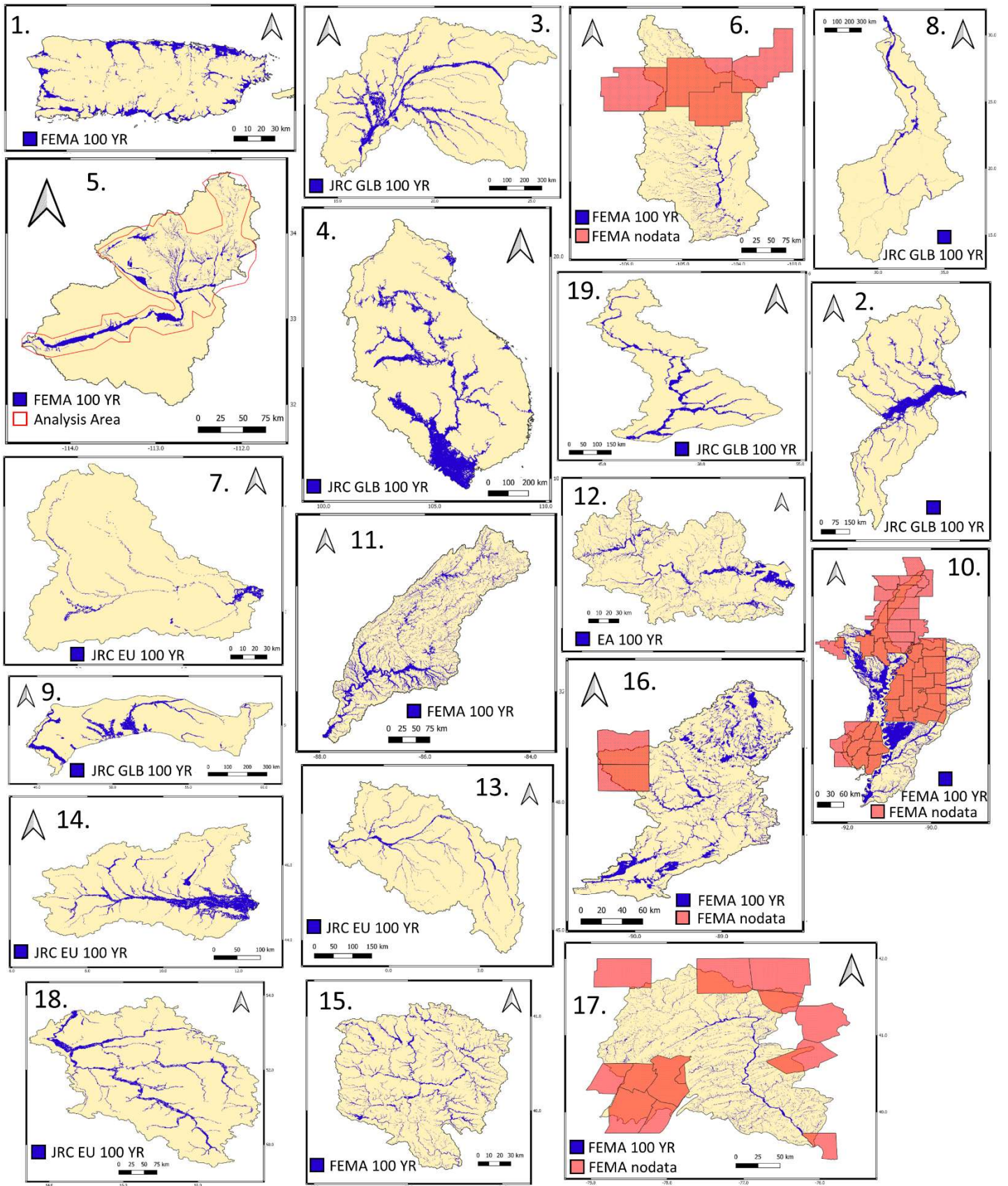


Figure S2. Visualization of the reference flood maps used for calibration in each of the calibration basins. Calibration basins are as follows: 1. Puerto Rico, 2. Central Amazon, 3. Lower Congo, 4. Lower Mekong, 5. Lower Gila, 6. Upper Pecos, 7. Jucar, 8. Upper Nile, 9. Lower Lena, 10. Lower Mississippi, 11. Alabama, 12. Thames, 13. Loire, 14. Po, 15. Muskingum, 16. Rock, 17. Susquehanna, 18. Oder, 19. Central Lena

Table S2. Performance Score Contingency Table

		Model	
		Wet	Dry
Reference	Wet	A – wet agreement	C – model underpredict
	Dry	B – model overpredict	D – dry agreement

Our method of model calibration aims to find the optimum Height Above Nearest Drainage value, H_N , for each Strahler stream order river that results in the best fit with the reference flood map. We use three different ‘fit’ statistics, derived from a contingency table (*Table S2*). The first score is the critical success index (CSI):

$$CSI = \frac{A}{A + B + C} \quad (S1)$$

CSI scores range from 1 (best) to 0 (worst). The second score is the hit rate (HR):

$$HR = \frac{A}{A + C} \quad (S2)$$

HR ranges from 1 (entire reference flood map captured) to 0 (none of the reference flood map captured). The third score is Bias:

$$Bias = \frac{A + B}{A + C} \quad (S3)$$

Bias scores <1 and >1 indicate a bias towards underprediction and overprediction, respectively.

Calibration was split into two stages. In the first stage, each river in the calibration basin was split by Strahler stream order and each order was processed individually. A range of permissible H_N values (typically the 5 H_N values resulting in bias scores close to 1) was found for each stream order. In the second calibration stage, the H_N ranges for each stream order were combined to produce maps with several different H_N combinations. Each of these combinations was then tested against the reference flood maps to find the optimal H_N combination for each climate zone.

In the first calibration stage, the river network was split into separate Strahler stream orders. Potential H_N values ranging from 0-20 m were tested for each Strahler stream order in each basin. H_N values that produced Bias scores closest to 1 (unbiased), hereafter referred to as $u-H_N$, were identified for each Strahler stream order. The $u-H_N$ values were then used as the basis for producing the permissible H_N ranges for each order. Ranges were initially chosen as $u-H_N \pm 2$. Some of the ranges were widened to match the ranges of the other calibration basins in the same climate zone. The final H_N ranges taken into part 2 of the calibration are listed in *Table S3*.

In the second calibration stage, flood maps were produced in each basin for all possible combinations of H_N within the pre-specified ranges. The only rule for H_N combinations was that a higher order stream’s H_N couldn’t be smaller than a lower order stream’s H_N ($H_{N-1} \leq H_N$). The number of different H_N combinations (or flood maps) tested varied between each basin and was dependent on how many Strahler stream orders were present in the basin. The total combinations tested for each basin are listed in *Table S3*. The Jucar river basin (ID 7) had the fewest combinations (758) while the Mississippi basin (ID 10) had the most (868,915). Scores were calculated to capture the level of fit between each flood map iteration and the reference flood map. CSI was the main score used for determining the best level of fit between the model and the reference map. Because only one H_N combination can be used to define the flood map in each climate zone, the optimal H_N combination across all calibration basins within the same climate zones were determined by iteratively applying CSI thresholds to each basin. From the small selection of H_N combinations remaining after this iterative process, the final combination chosen was the one that resulted in the highest average CSI across the basins. Final H_N values for each climate zone are presented in *Table S4*.

Table S3. H_N ranges for Calibration Stage 2 for each basin in each climate zone. Basin IDs correspond with Figure S1

	Basin ID									
Order	1	2	3	4	5	6	7	8	9	10
1	0-4 m				0-4 m	0-4 m				0-2 m
2	0-5 m				0-4 m	0-4 m				0-3 m
3	0-5 m				0-4 m	0-4 m				0-6 m
4	3-8 m				0-5 m	0-5 m	0-5 m			0-9 m
5	2-13 m		2-13 m		0-7 m	0-7 m	0-7 m			2-11 m
6		3-13 m	3-13 m	3-13 m	1-8 m	1-8 m	1-8 m	1-8 m	1-8 m	3-12 m
7		3-13 m	3-13 m	3-13 m		2-10 m	2-10 m	2-10 m	2-10 m	5-13 m
8		3-13 m	3-13 m	3-13 m				2-10 m	2-10 m	7-13 m
9			7-17 m	7-17 m	2-14 m			2-14 m	2-14 m	7-13 m
10			7-17 m	7-17 m	5-15 m			5-15 m		9-14 m
11		7-17 m							9-15 m	
Combinations	2220	1890	38756	9426	84504	7726	758	7899	7088	868915
	Basin ID									
Order	11	12	13	14	15	16	17	18	19	
1	0-2 m	0-2 m			0-2 m	0-2 m	0-2 m			
2	0-3 m	0-3 m			0-2 m	0-2 m	0-2 m			
3	0-6 m	0-6 m			0-5 m	0-5 m	0-5 m			
4	0-9 m	0-9 m	0-9 m	0-9 m	2-7 m	2-7 m	2-7 m	2-7 m		
5	2-11 m	2-11 m	2-11 m	2-11 m	2-10 m	2-10 m	2-10 m	2-10 m		
6	3-12 m	3-12 m	3-12 m	3-12 m	4-13 m	4-13 m	4-13 m	4-13 m	4-13 m	
7	5-13 m		5-13 m	5-13 m	5-14 m	5-14 m	5-14 m	5-14 m	5-14 m	
8			7-13 m	7-13 m			6-16 m	6-16 m		
9			7-13 m					7-16 m		
10									8-16 m	
11									8-16 m	
Combinations	33576	7733	17172	6283	26728	26728	148340	29443	1280	

Table S4. Final H_N Values for RFSM

	Maximum Height Above Nearest Drainage (H_N)			
Order	Tropical	Arid	Temperate	Continental
1	1 m	0 m	0 m	0 m
2	2 m	0 m	1 m	0 m
3	4 m	0 m	2 m	2 m
4	6 m	1 m	4 m	4 m
5	8 m	3 m	5 m	5 m
6	8 m	3 m	7 m	6 m
7	9 m	5 m	9 m	8 m
8	10 m	5 m	10 m	9 m
9	10 m	12 m	10 m	10 m
10	10 m	13 m	13 m	11 m
11	13 m	14 m	-	12 m

S2 Model Validation

Validation of the RFSM was split into two stages. The first stage compared the RFSM to existing global flood model (GFM) outputs in Africa. The performance of the RFSM with respect to these existing GFMs was compared with the performance of another global geomorphological floodplain map: GFPLAIN250 (Nardi et al., 2019). The second stage involved validating the RFSM output against historical observed flood events. The performance of the RFSM at capturing these historical events was compared with the performance of existing GFMs.

S2.1 Validation Against Existing Models

The output of 6 GFMs was compared in Africa by Trigg et al. (2016b) in the first GFM intercomparison study. One of the outputs of the study was an aggregated map (Trigg et al., 2016a) of flood hazard for Africa that showed the number of models (1-6) that agreed it would flood in a given location (see *Figure S3*). We use this aggregated map to validate our RFSM. We also validate another geomorphological flood map, GFPLAIN250 (Nardi et al., 2019), against the aggregated GFM map. We then compare the results to see how our approach compares to geomorphological approaches. We use the 100-year return period aggregated GFM map for our validation.

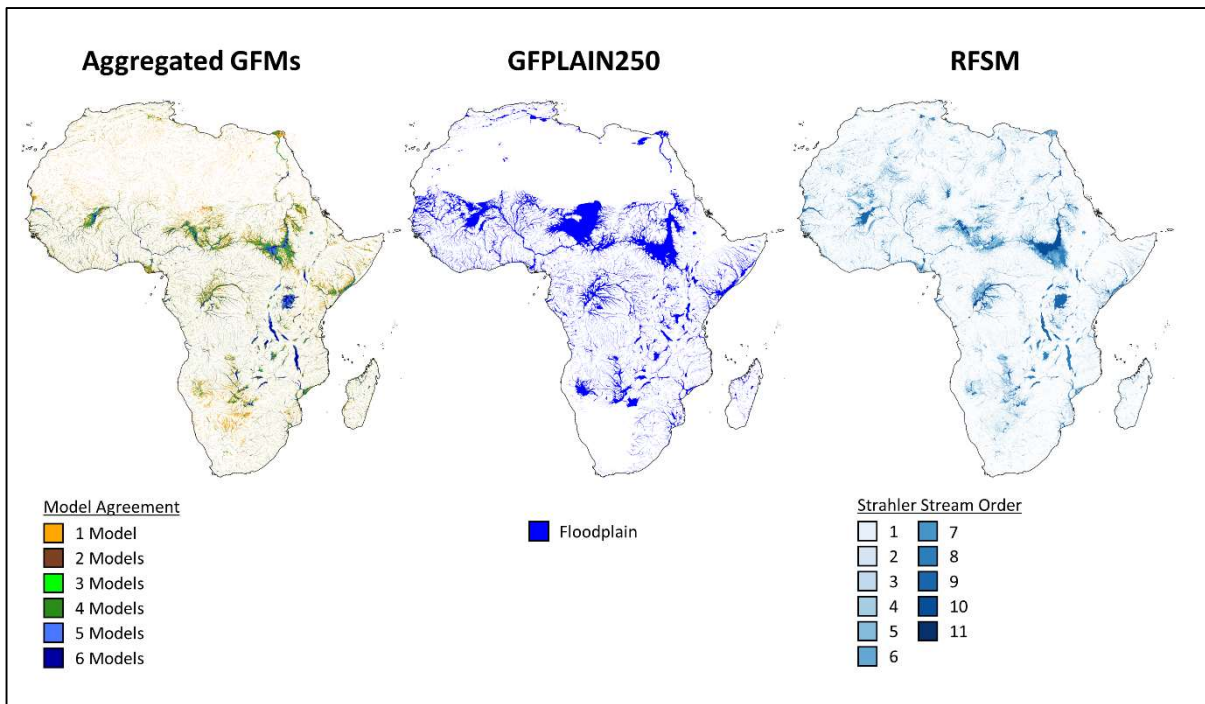


Figure S3. Datasets used in the validation. (From left to right) 100-year return period aggregated global flood model output for Africa (Trigg et al., 2016a). GFPLAIN250 geomorphological floodplain map for Africa (Nardi et al., 2019). RFSM map with rivers split by their Strahler stream orders.

Comparison of the RFSM map with the aggregated GFM map is split into three parts. In the first part, we split the RFSM map into Strahler stream orders. We then overlay the entire aggregated GFM map (any level of agreement) with the RFSM map and calculated the percentage of each Strahler stream order's extent that is overpredicting flooding with respect to the aggregated GFM map:

$$\% OP_{order} = \frac{RFSM_{order} - (RFSM_{order} \cap AGG)}{RFSM_{order}} \times 100 \quad (S4)$$

where $RFSM_{order} \cap AGG$ is the intersection of the RFSM map (of a given order) and the aggregated GFM map, and $RFSM_{order}$ is the total extent of the RFSM map at that order.

In the second part of the analysis, we split the aggregated GFM map into its different levels of agreement, ranging from 1-6. We then calculate, for each level of agreement, the percentage of the aggregated GFM map that is captured by both the RFSM map and the GFPLAIN250 map:

$$\% \text{ Captured}_{agg \text{ level}} = \frac{GFM_{agg \text{ level}} \cap FM}{GFM_{agg \text{ level}}} \times 100 \quad (S5)$$

where $GFM_{agg \text{ level}} \cap FM$ is the intersection of the aggregated GFM map (at the specified agreement level) and the flood map (either RFSM or GFPLAIN250) and $GFM_{agg \text{ level}}$ is the total aggregated GFM extent for the specified agreement level.

In the third part of the analysis, the RFSM map and GFPLAIN250 maps were scored using the performance scores outlined in the calibration section (equations S1-S3). To make the comparison between the RFSM map and the GFPLAIN250 as fair as possible an upstream drainage area (UDA) threshold of 1000 km² was applied to the RFSM

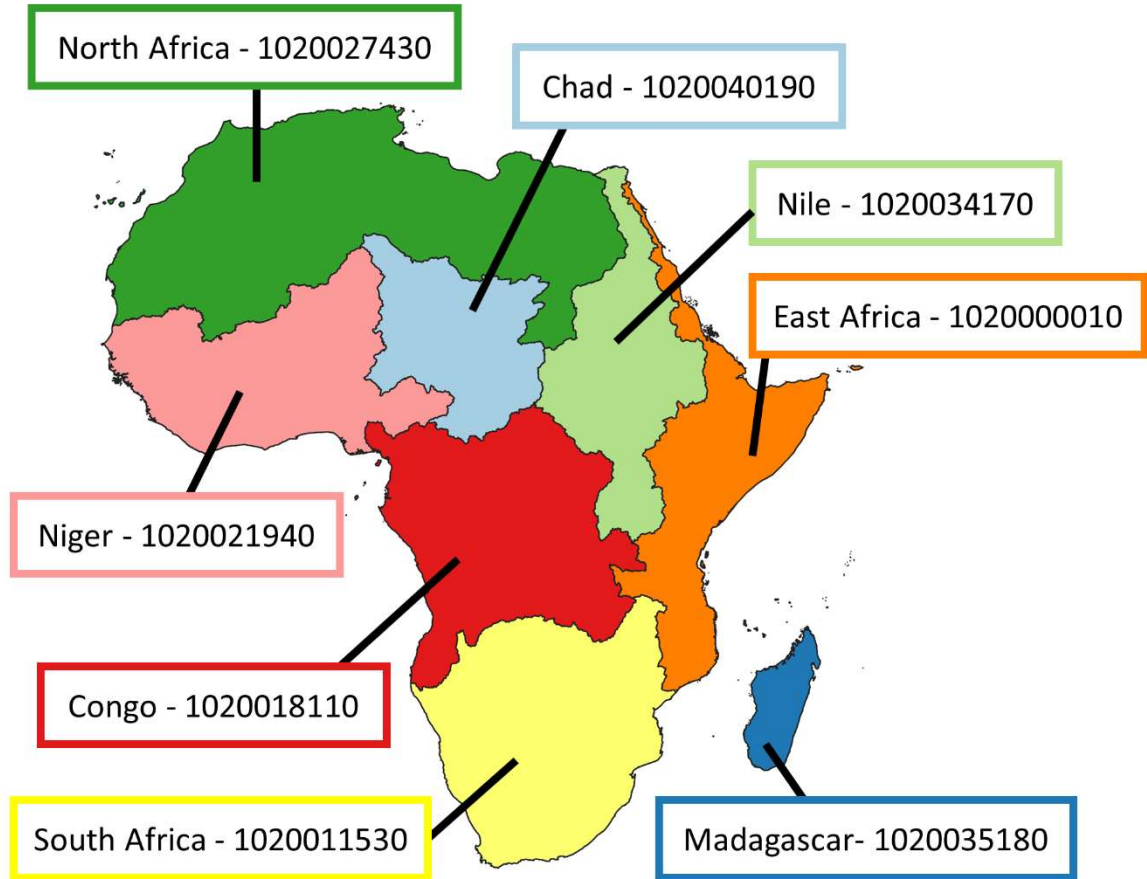


Figure S4. The level 2 HydroBasins used for validation. Basin names listed alongside HydroBasin specific numeric codes.

map. This is because GFPLAIN250 does not map rivers below this threshold (Nardi et al., 2019). Performance scores were calculated by intersecting the GFPLAIN250 and RFSM maps with the aggregated GFM map, with 6 different thresholds of agreement applied to the aggregated GFM map. These thresholds of agreement ranged from ≥ 1 model (where any model predicting flooding) to 6 models (where all 6 models agree it will flood).

The African continent was split into major drainage basins for this first stage of validation. We use the HydroBasins dataset (Lehner and Grill, 2013) at the level 2 categorization as our validation basins. The basin split for the continent of Africa can be seen in Figure S4, alongside basin names and HydroBasin specific numeric codes. For the continent of Africa there are a total of 8 level 2 basins. The three parts of the validation analysis outlined above were carried out in each of the 8 basins. Results for validation parts 1-3 are recorded in Tables S5 - S9. Figures S5-S12 visualize the overlap between both the RFSM and GFPLAIN250 maps and the aggregated GFM map for each of the 8 level 2 basins.

Table S5 - Validation Part 1 Results - RFSM Percentage Oveprediction per Stream Order

Basin	Strahler Stream Order										
	1	2	3	4	5	6	7	8	9	10	11
East Africa - 1020000010	83	80	69	49	31	14	11	5	4	14	X
South Africa - 1020011530	86	83	74	55	37	19	13	6	2	16	X
Congo - 1020018810	91	91	74	49	32	16	11	9	4	4	7
Niger - 1020021940	81	91	77	64	32	14	23	16	10	2	X
North Africa - 1020027430	94	96	93	88	77	65	62	61	68	X	X
Nile - 1020034170	84	80	71	55	40	29	20	13	2	5	X
Madagascar - 1020035180	83	85	68	45	22	6	3	1	X	X	X
Chad - 1020040190	86	82	77	61	48	34	31	19	33	1	X

Throughout Africa, the RFSM follows the general trend that as the Strahler stream order of the river increases, the degree of overprediction decreases (*Table S5*). Low orders (1, 2 and 3) have high degrees of overprediction. This is because the RFSM has a smaller minimum UDA threshold (10 km²) than any of the other GFM (between 50-5000 km²) and a lot of the rivers in these categories fall below the minimum upstream drainage area threshold of any GFM. Intermediate orders (4-6) still show some levels of overprediction as a lot of these rivers will be modelled by some, but not all, of the GFMs. The levels of overprediction decrease for higher order rivers (>7) for which there is complete coverage across the GFMs.

Table S6 - Validation Part 2 Results - Percentage Flooding Captured per GFM Agreement Level

Basin	Flood Map	GFM Agreement Level					
		1	2	3	4	5	6
East Africa - 1020000010	RFSM	34	52	67	78	87	94
	GFPLAIN250	25	51	66	76	79	73
South Africa - 1020011530	RFSM	43	59	73	83	93	98
	GFPLAIN250	20	43	58	71	74	63
Congo - 1020018110	RFSM	50	58	73	84	93	98
	GFPLAIN250	33	58	72	79	77	68
Niger - 1020021940	RFSM	52	69	83	91	96	98
	GFPLAIN250	44	69	85	93	97	97
North Africa - 1020027430	RFSM	46	62	74	82	90	93
	GFPLAIN250	16	27	46	62	80	92
Nile - 1020034170	RFSM	61	78	88	94	98	99
	GFPLAIN250	49	73	84	83	65	55
Madagascar - 1020035180	RFSM	38	42	63	80	91	96
	GFPLAIN250	12	31	48	60	74	80
Chad - 1020040190	RFSM	56	73	84	89	92	95
	GFPLAIN250	60	76	86	93	97	99

In *Part 2* of the validation, we look at the different levels of GFM agreement in the aggregated GFM map and examine the percentage of each agreement level that is captured by the RFSM and GFPLAIN250 maps (*Table S6*). The higher the GFM agreement level, the greater the confidence that it will flood in a given location. As such, it is especially important that the models being tested correctly capture these areas of high agreement. For the two highest GFM agreement levels (5 models agree, and 6 models agree) the RFSM has a % *captured* value of above 90% in each basin in Africa. This shows that the RFSM map is correctly capturing these areas of high confidence of flooding. Comparing the % *captured* results of the RFSM with the GFPLAIN250 map, the RFSM has higher % *captured* results in each basin except the Chad basin (where both maps still score highly). This shows that the RFSM captures more of aggregated GFM extent than the GFPLAIN250 map.

Table S7 - Validation Part 3 Results - Critical Success Index Scores for each GFM Agreement Threshold

Basin	Flood Map	GFM Agreement Threshold					
		≥1	≥2	≥3	≥4	≥5	6
East Africa - 1020000010	RFSM	0.31	0.46	0.47	0.41	0.31	0.14
	GFPLAIN250	0.35	0.36	0.29	0.21	0.14	0.07
South Africa - 1020011530	RFSM	0.35	0.5	0.49	0.43	0.34	0.22
	GFPLAIN250	0.33	0.36	0.31	0.24	0.17	0.1
Congo - 1020018110	RFSM	0.44	0.56	0.56	0.49	0.38	0.22
	GFPLAIN250	0.45	0.44	0.36	0.28	0.19	0.1
Niger - 1020021940	RFSM	0.47	0.54	0.5	0.39	0.27	0.14
	GFPLAIN250	0.48	0.43	0.33	0.24	0.15	0.08
North Africa - 1020027430	RFSM	0.21	0.13	0.06	0.03	0.01	0.003
	GFPLAIN250	0.15	0.12	0.07	0.04	0.02	0.01
Nile - 1020034170	RFSM	0.59	0.61	0.54	0.44	0.31	0.13
	GFPLAIN250	0.52	0.45	0.35	0.24	0.15	0.06
Madagascar - 1020035180	RFSM	0.27	0.42	0.51	0.5	0.37	0.19
	GFPLAIN250	0.32	0.42	0.41	0.34	0.24	0.12
Chad - 1020040190	RFSM	0.4	0.39	0.31	0.21	0.13	0.06
	GFPLAIN250	0.41	0.29	0.19	0.12	0.07	0.03

Table S8 - Validation Part 3 Results - Hit Rate Scores for each GFM Agreement Threshold

Basin	Flood Map	GFM Agreement Threshold					
		≥1	≥2	≥3	≥4	≥5	6
East Africa - 1020000010	RFSM	0.32	0.54	0.68	0.78	0.85	0.9
	GFPLAIN250	0.45	0.65	0.73	0.76	0.76	0.73
South Africa - 1020011530	RFSM	0.37	0.62	0.76	0.87	0.93	0.97
	GFPLAIN250	0.39	0.58	0.65	0.69	0.67	0.63
Congo - 1020018110	RFSM	0.47	0.67	0.79	0.88	0.94	0.97
	GFPLAIN250	0.55	0.69	0.73	0.74	0.72	0.68
Niger - 1020021940	RFSM	0.51	0.71	0.83	0.9	0.95	0.97
	GFPLAIN250	0.68	0.84	0.92	0.96	0.97	0.97
North Africa - 1020027430	RFSM	0.36	0.53	0.67	0.76	0.82	0.85
	GFPLAIN250	0.22	0.37	0.56	0.7	0.83	0.92
Nile - 1020034170	RFSM	0.65	0.8	0.89	0.94	0.97	0.98
	GFPLAIN250	0.65	0.73	0.72	0.68	0.61	0.55
Madagascar - 1020035180	RFSM	0.28	0.45	0.61	0.74	0.85	0.91
	GFPLAIN250	0.34	0.51	0.62	0.7	0.77	0.8
Chad - 1020040190	RFSM	0.49	0.64	0.73	0.79	0.83	0.86
	GFPLAIN250	0.74	0.85	0.92	0.95	0.98	0.99

Table S9 - Validation Part 3 Results - Bias Scores for each GFM Agreement Threshold

Basin	Flood Map	GFM Agreement Threshold					
		≥1	≥2	≥3	≥4	≥5	6
East Africa - 1020000010	RFSM	0.36	0.72	1.1	1.66	2.65	5.35
	GFPLAIN250	0.73	1.46	2.24	3.34	5.36	10.94
South Africa - 1020011530	RFSM	0.42	0.86	1.29	1.87	2.68	4.4
	GFPLAIN250	0.58	1.19	1.78	2.58	3.69	6.06
Congo - 1020018110	RFSM	0.52	0.86	1.2	1.66	2.42	4.32
	GFPLAIN250	0.76	1.25	1.75	2.42	3.53	6.3
Niger - 1020021940	RFSM	0.6	1.1	1.5	2.21	3.46	7.06

	GFPLAIN250	1.09	1.83	2.71	4	6.27	12.79
North Africa - 1020027430	RFSM	1.03	3.51	10.03	25.6	69.3	266.4
	GFPLAIN250	0.71	2.45	7	17.87	48.36	185.89
Nile - 1020034170	RFSM	0.75	1.13	1.53	2.09	3.08	3.63
	GFPLAIN250	0.89	1.33	1.81	2.47	7.66	9.05
Madagascar - 1020035180	RFSM	0.29	0.52	0.81	1.24	2.13	2.96
	GFPLAIN250	0.41	0.72	1.13	1.73	4.82	6.71
Chad - 1020040190	RFSM	0.71	1.3	2.14	3.54	6.24	14.2
	GFPLAIN250	1.55	2.83	4.66	7.73	13.63	31

In the *Part 3* of the validation the same UDA threshold as the GFPLAIN250 map (1000 km²) was applied to the RFSM map. Three different performance scores were then calculated for both of these maps in each basin in Africa. In terms of CSI (*Table S7*), the RFSM map outperformed the GFPLAIN250 map in almost all the basins in Africa. The bias scores (*Table S9*) for the GFPLAIN250 map were also higher than the RFSM map's bias scores, suggesting that GFPLAIN250 overpredicts the 100-year flood to a greater degree than the RFSM map.

It should be noted that the GFPLAIN250 map was not intended to map the '100-year' flood, but rather to identify floodplain boundaries (Nardi et al., 2019). Additionally, in the North Africa basin, which contains the majority of the Sahara desert, GFPLAIN250 and a few of the global flood models apply masks that exclude these areas from the analysis. This explains the low validation scores in this basin with respect to the other basins in Africa. We chose not to apply any mask in these areas for two reasons. Firstly, there is little to no population in these areas, so applying / not applying a mask would have little impact on the final results. Secondly, applying a mask could mistakenly remove areas that do contain rivers. This is evident in the Nile Basin in *Figure S10*. The mask applied to the GFPLAIN250 removes a portion of the Nile River in Northern Sudan.

We have shown, in our validation of the RFSM against the aggregated output of six GFMs, that the RFSM does a good job at capturing areas where there is high agreement between the GFMs. It also does a better job at predicting the 100-year flood extent than existing global geomorphological floodplain datasets.

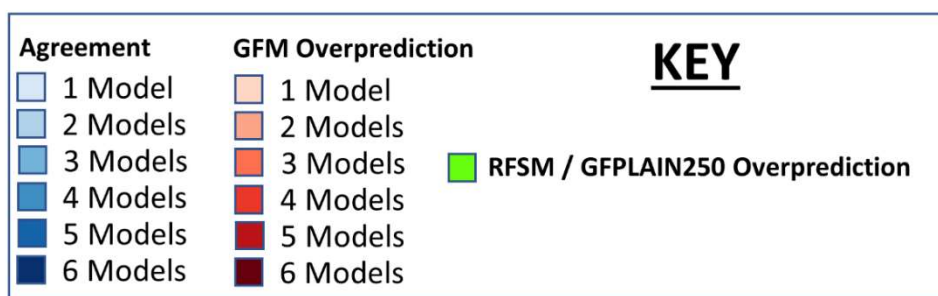
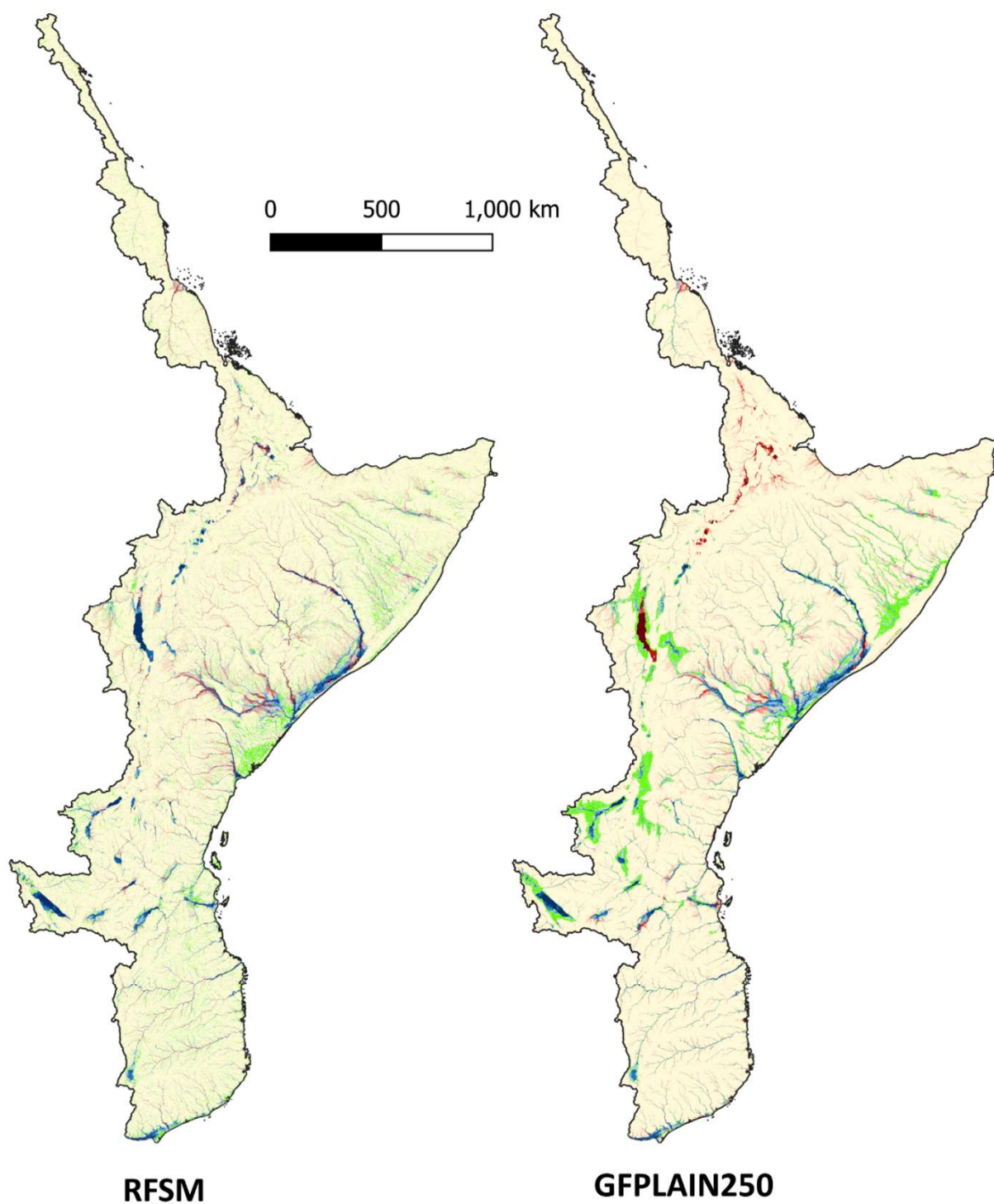


Figure S5. Overlap of the RFSM and GFPLAIN250 maps with the 100-year return period aggregated global flood model map (Trigg et al., 2016a) in the East Africa Basin (1020000010).

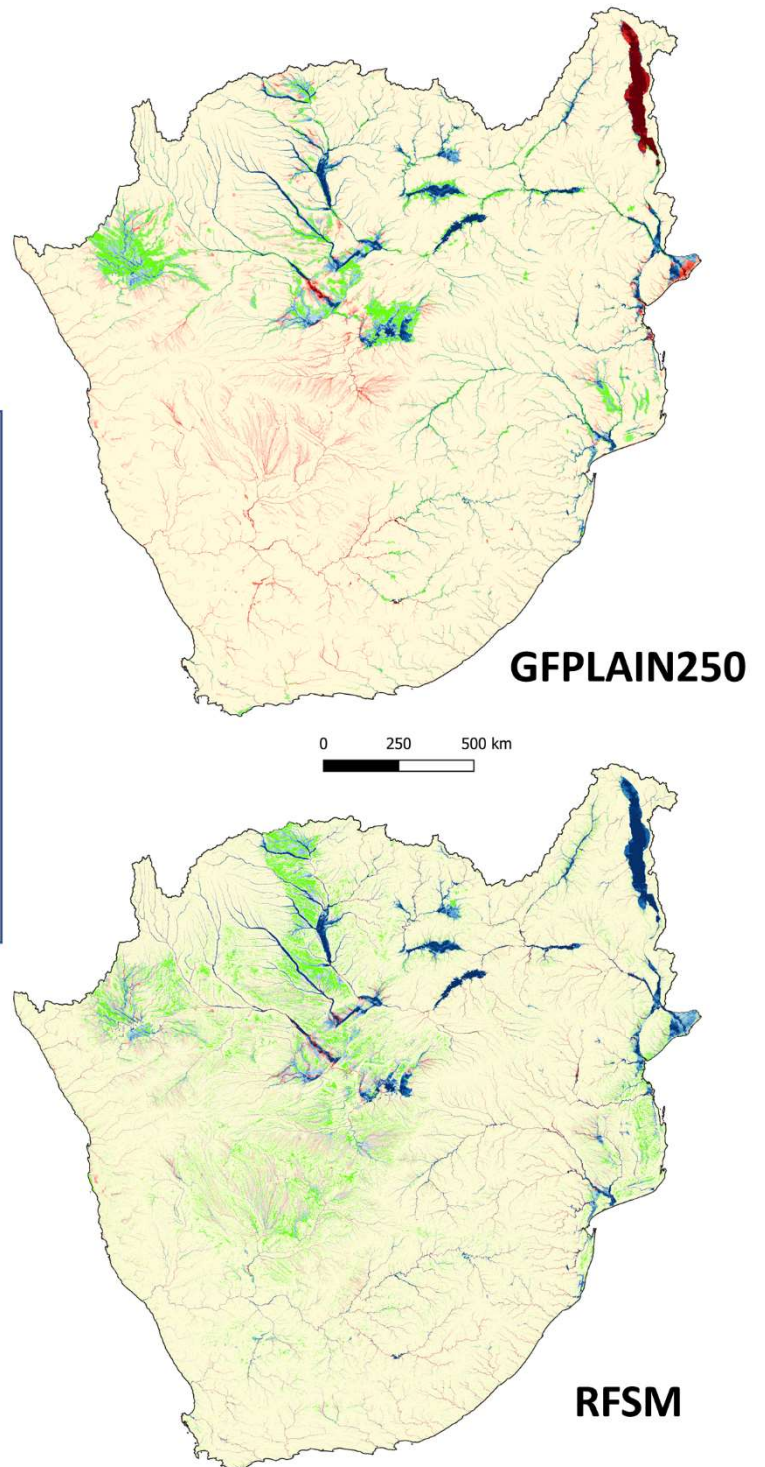
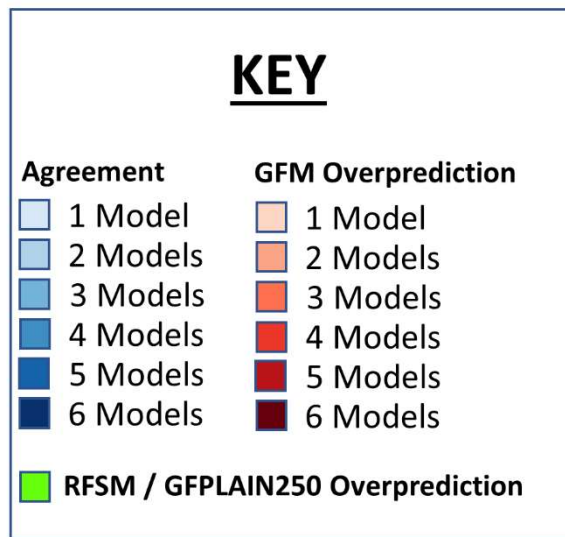


Figure S6. *Overlap of the RFSM and GFPLAIN250 maps with the 100-year return period aggregated global flood model map (Trigg et al., 2016a) in the South Africa Basin (1020011530).*

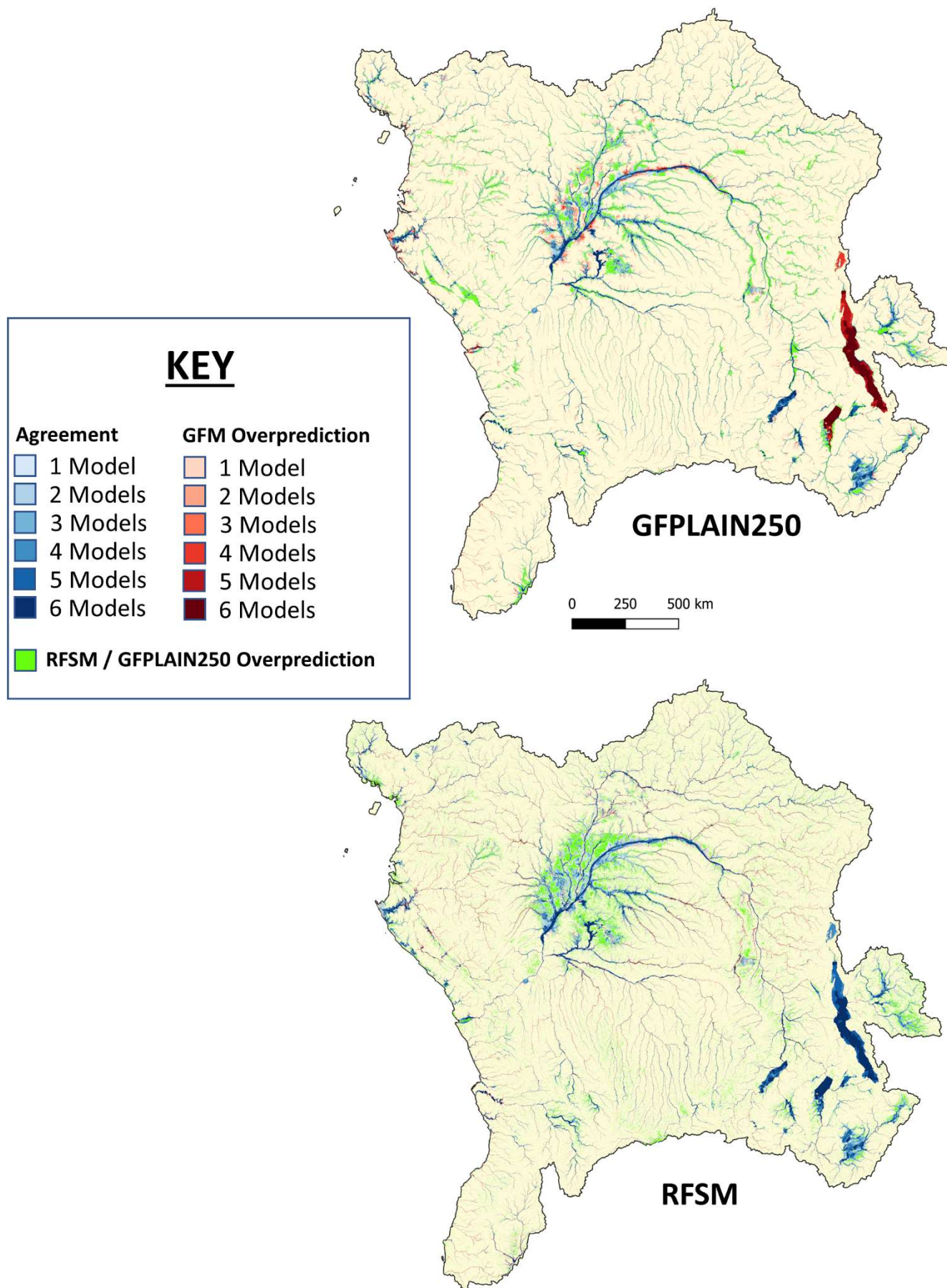
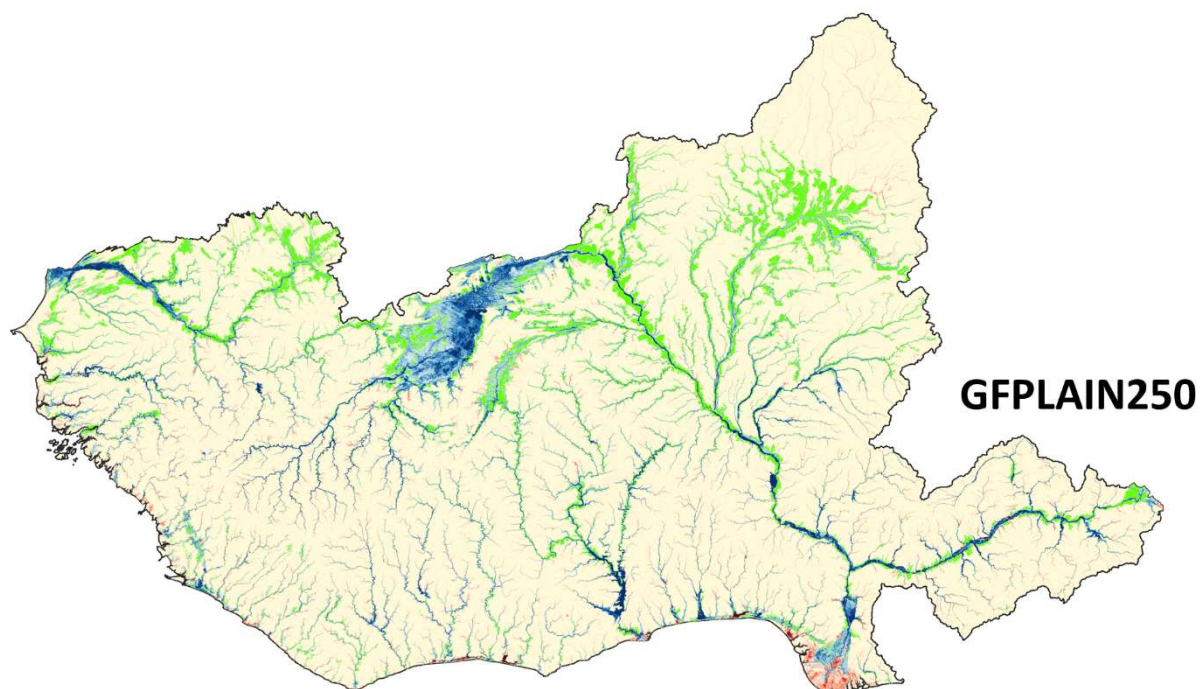


Figure S7. Overlap of the RFSM and GFPLAIN250 maps with the 100-year return period aggregated global flood model map (Trigg et al., 2016a) in the Congo Basin (1020018110).



0 250 500 km

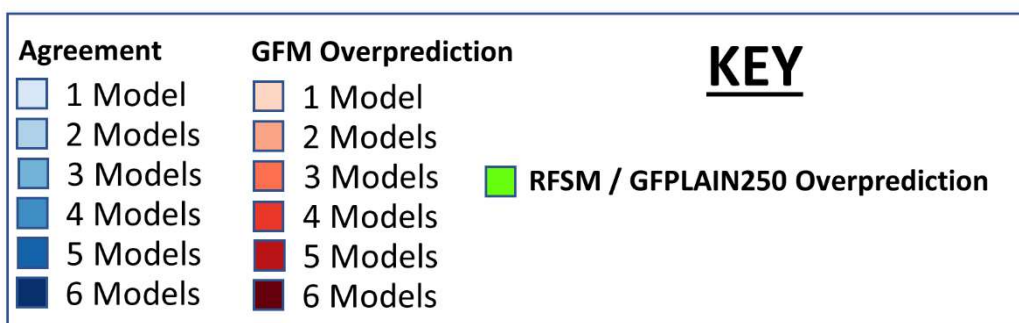
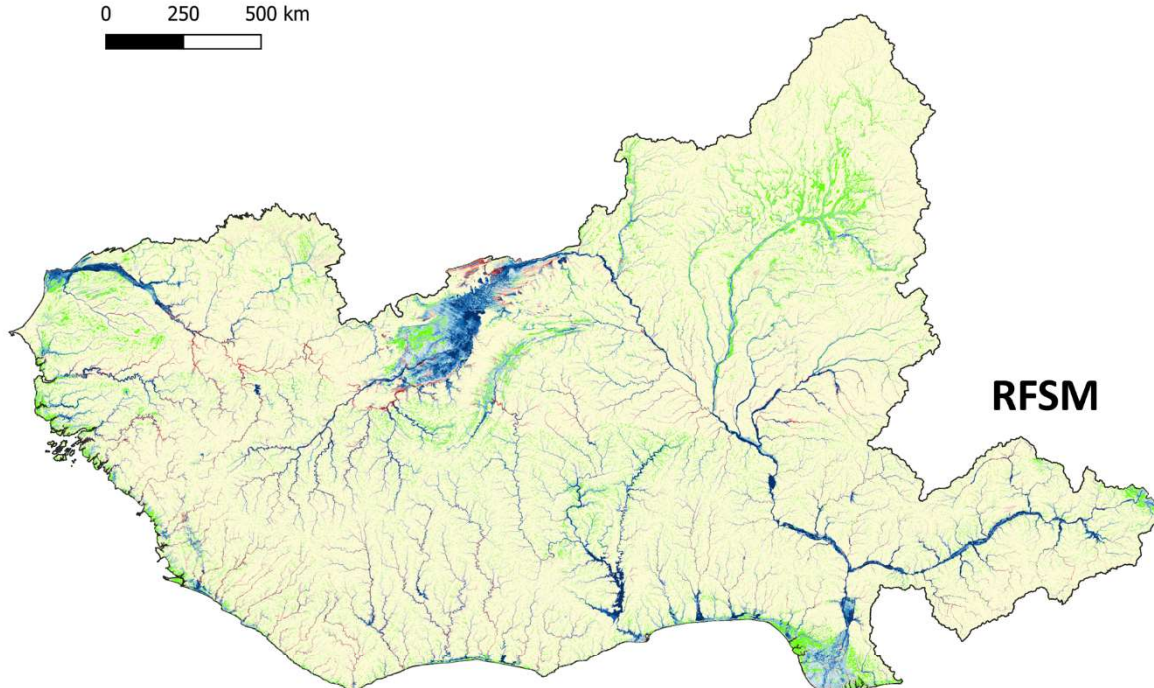


Figure S8. Overlap of the RFSM and GFPLAIN250 maps with the 100-year return period aggregated global flood model map (Trigg et al., 2016a) in the Niger Basin (1020021940).

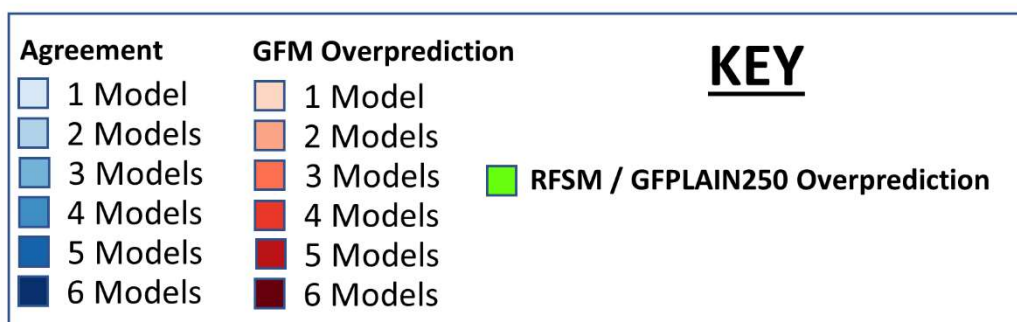
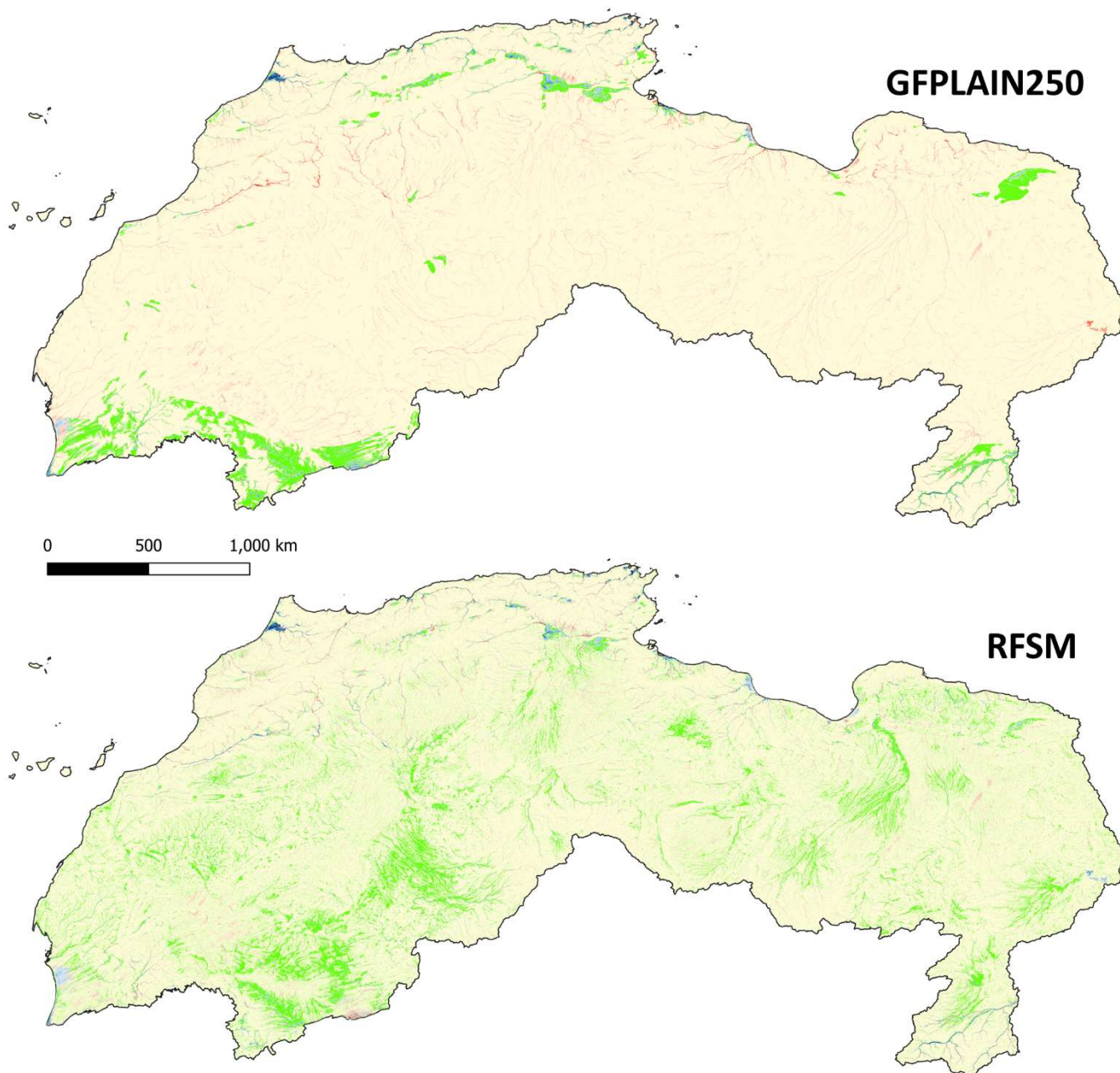


Figure S9. Overlap of the RFSM and GFPLAIN250 maps with the 100-year return period aggregated global flood model map (Trigg et al., 2016a) in the North Africa Basin (1020027430).

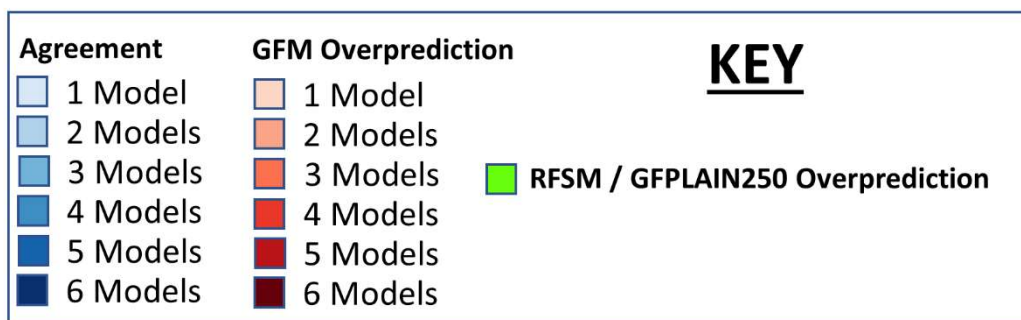
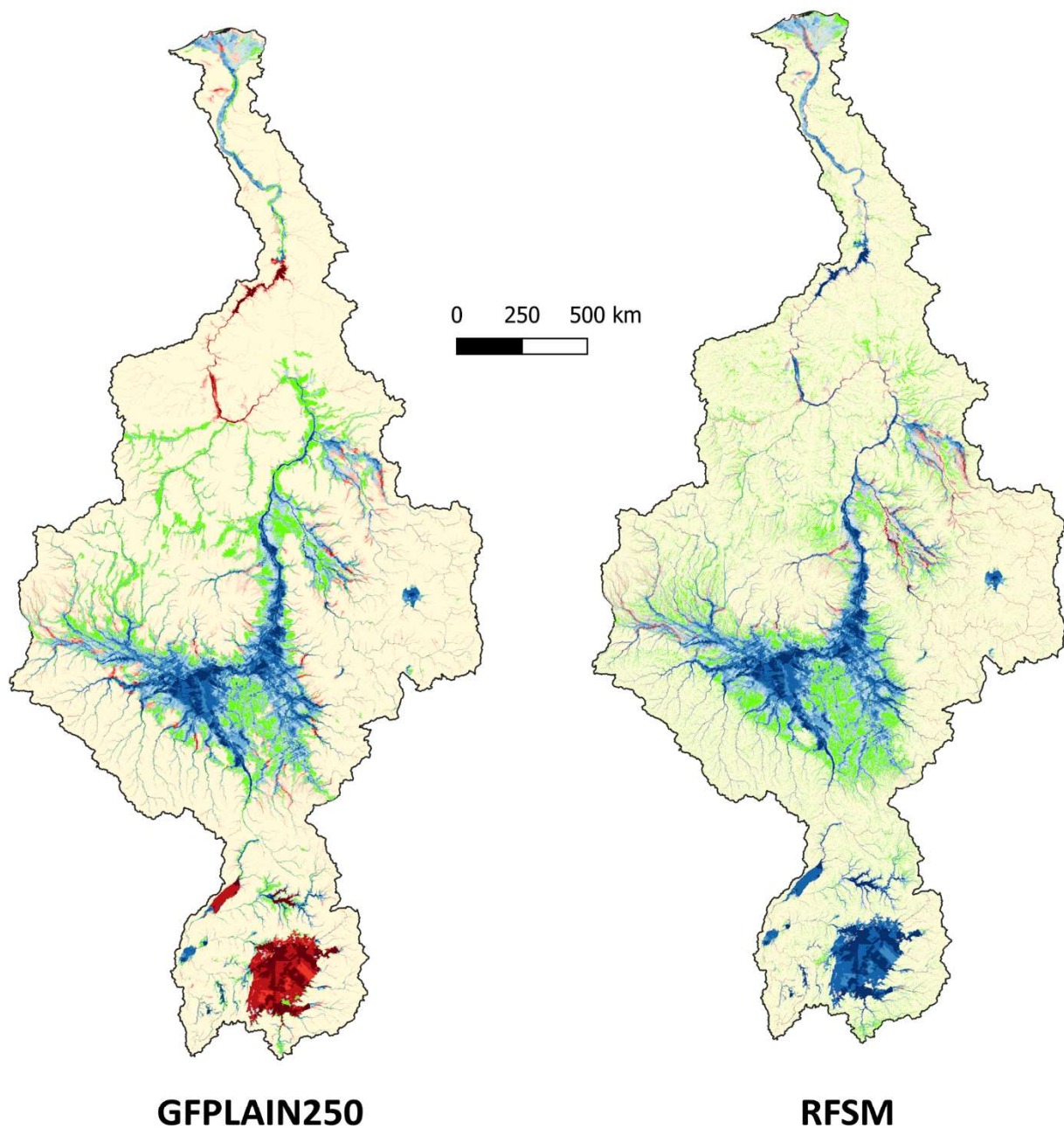


Figure S10. Overlap of the RFSM and GFPLAIN250 maps with the 100-year return period aggregated global flood model map (Trigg et al., 2016a) in the Nile Basin (1020034170).

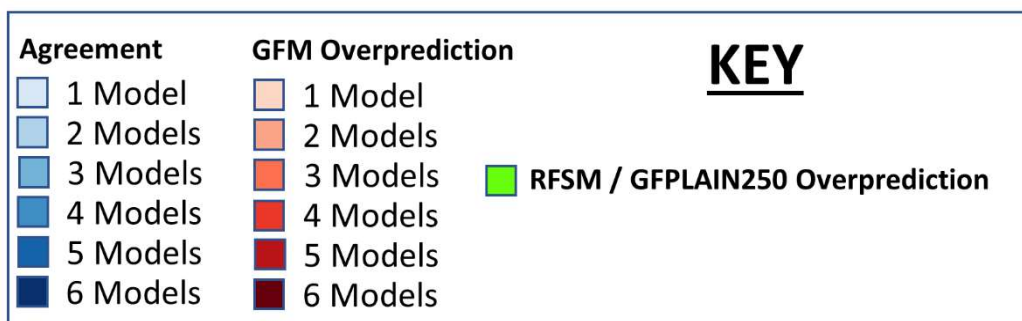
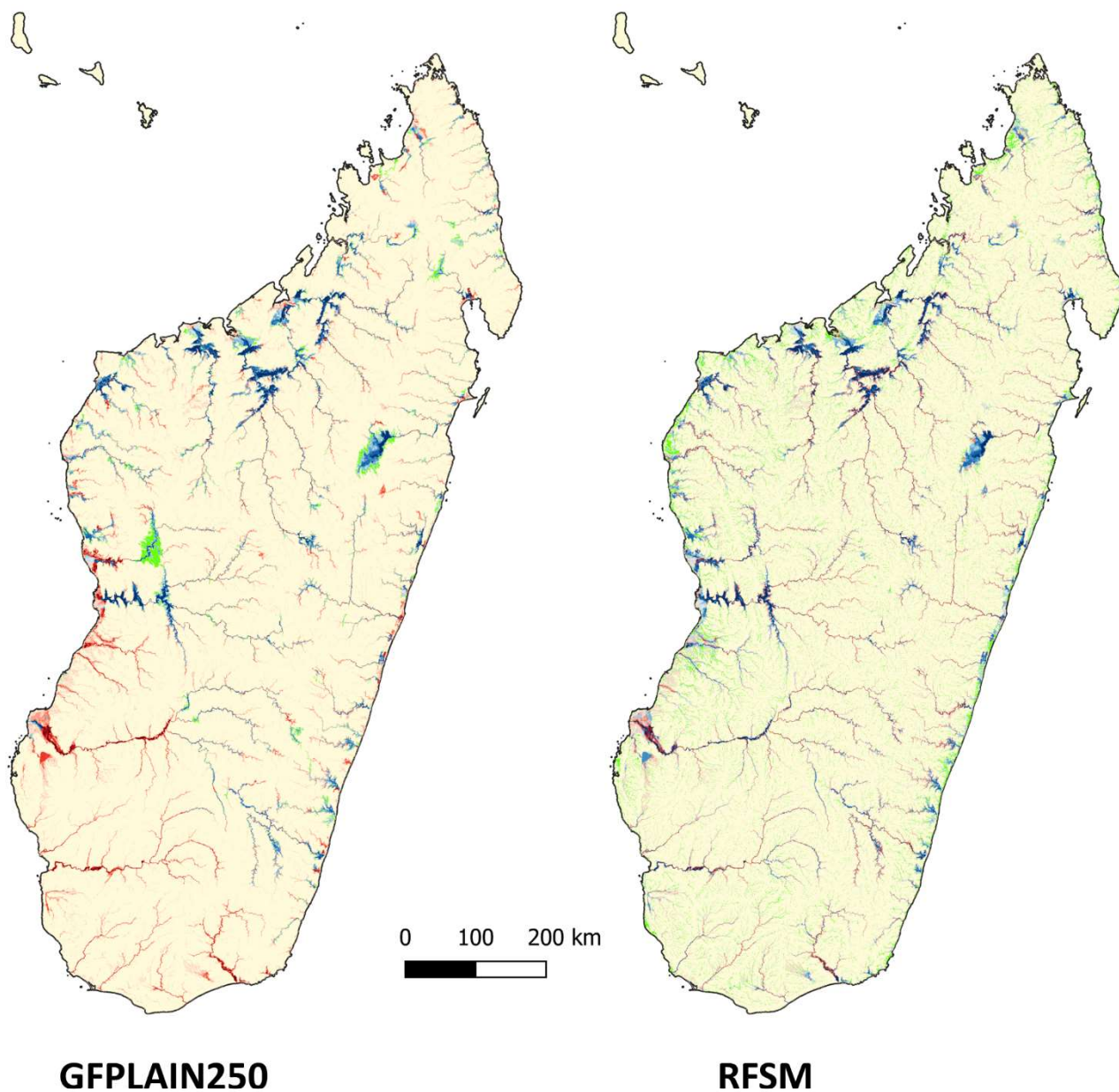


Figure S11. Overlap of the RFSM and GFPLAIN250 maps with the 100-year return period aggregated global flood model map (Trigg et al., 2016a) in the Madagascar Basin (1020035180).

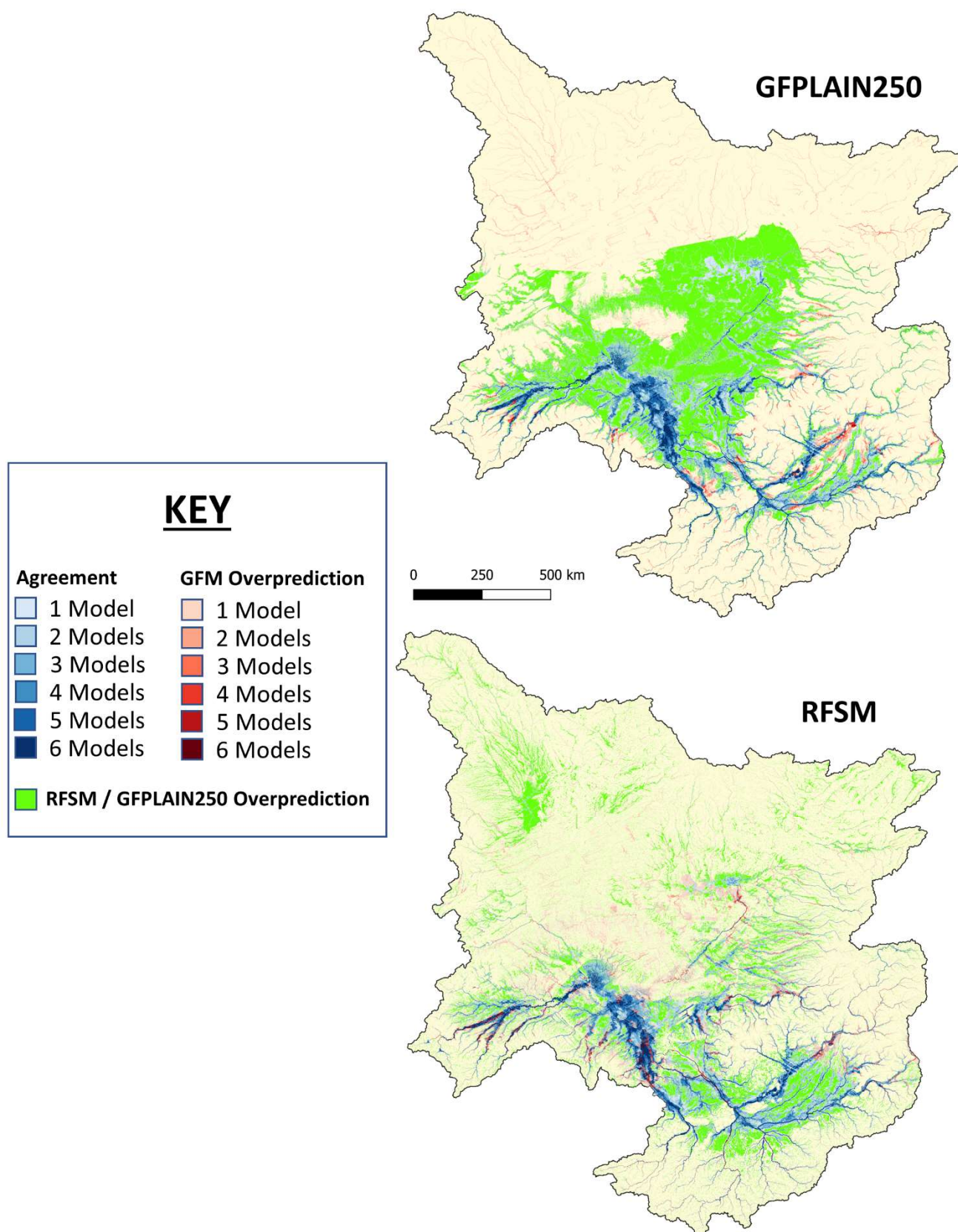


Figure S12. Overlap of the RFSM and GFPLAIN250 maps with the 100-year return period aggregated global flood model map (Trigg et al., 2016a) in the Chad Basin (1020040190).

S2.2 Validation Against Observed Events

In a follow up study to the Trigg et al. (2016b) GFM intercomparison study, Bernhofen et al. (2018b) did a comparative validation of 6 GFMs against observed flood events in Nigeria and Mozambique. The two flood events used for validation were the 2012 floods in Nigeria and the 2007 floods in Mozambique. Validation was split into three hydraulically diverse analysis regions: two in Nigeria and one in Mozambique. The analysis areas in Nigeria were Lokoja, which is a narrow, confined floodplain that sits at the confluence of the Niger and Benue rivers; and Idah, which sits downstream of Lokoja and is a flat extensive floodplain. The analysis area in Mozambique is Chemba, which is a multichannel portion of the lower Zambezi river. Six global flood models were tested in total, GLOFRIS (Winsemius et al., 2013), JRC (Dottori et al., 2016c), U-Tokyo (Winsemius et al., 2013), ECMWF (Pappenberger et al., 2012), CIMA-UNEP (Rudari et al., 2015), and Fathom (Sampson et al., 2015). The study found varied performance between the GFMs, with some models scoring very well and others not very well (Bernhofen et al., 2018b).

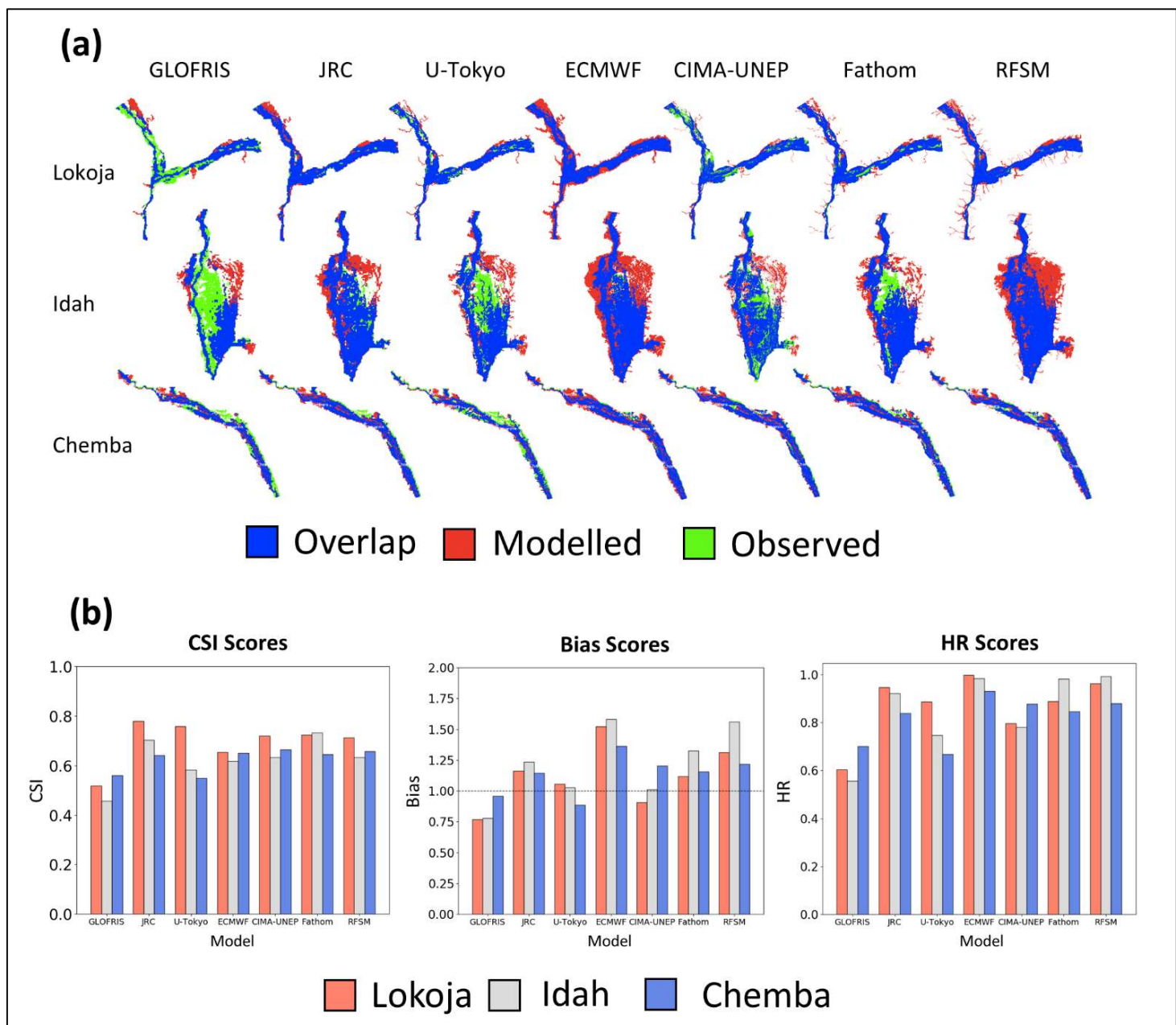


Figure S13. (a) Overlap of modelled 100-year flood extent and observed flood events in the three validation regions for 6 global flood models and the RFSM. (b) Performance scores for 6 global flood models and the RFSM in the three validation regions. Figure adjusted from Bernhofen et al. (2018b).

Here, we use the validation outputs from Bernhofen et al. (2018a) to see how the RFSM map compares when validated against the same observed flood events as six other GFMs. We use the three performance scores outlined in the Calibration section (*equations S1-S3*). These are the same scores used in the Bernhofen et al. (2018b) study. We use the 100-year return period extents for each of the six GFMs for our validation. The overlap between the models and the observed events can be visualized in *Figure S13a* and the performance scores for each of the models can be visualized graphically in *Figure S13b*.

Across the three study regions, the RFSM consistently scores amongst the best GFMs in terms of CSI. In Chemba, the RFSM CSI score is the higher than any of the GFMs. In both basins in Nigeria, the RFSM has the second highest Bias score. The low river initiation threshold of the RFSM map (10 km² UDA) contributes to this overprediction. You can see in *Figure S13a* that a number of tributaries are included in Lokoja on which there is no flooding. Similarly, in Idah several floodplain channels not modelled by the other GFMs are represented in the RFSM, resulting in a larger flood extent and higher overprediction within the floodplain.

We've shown that the RFSM map performs similarly to the best performing GFMs when validated against historical flood events in three regions in Nigeria and Mozambique. This indicates that the RFSM does a good job of mapping the flood susceptibility of rivers and is appropriate for use in this study.

S3 Top 50 Countries Exposure

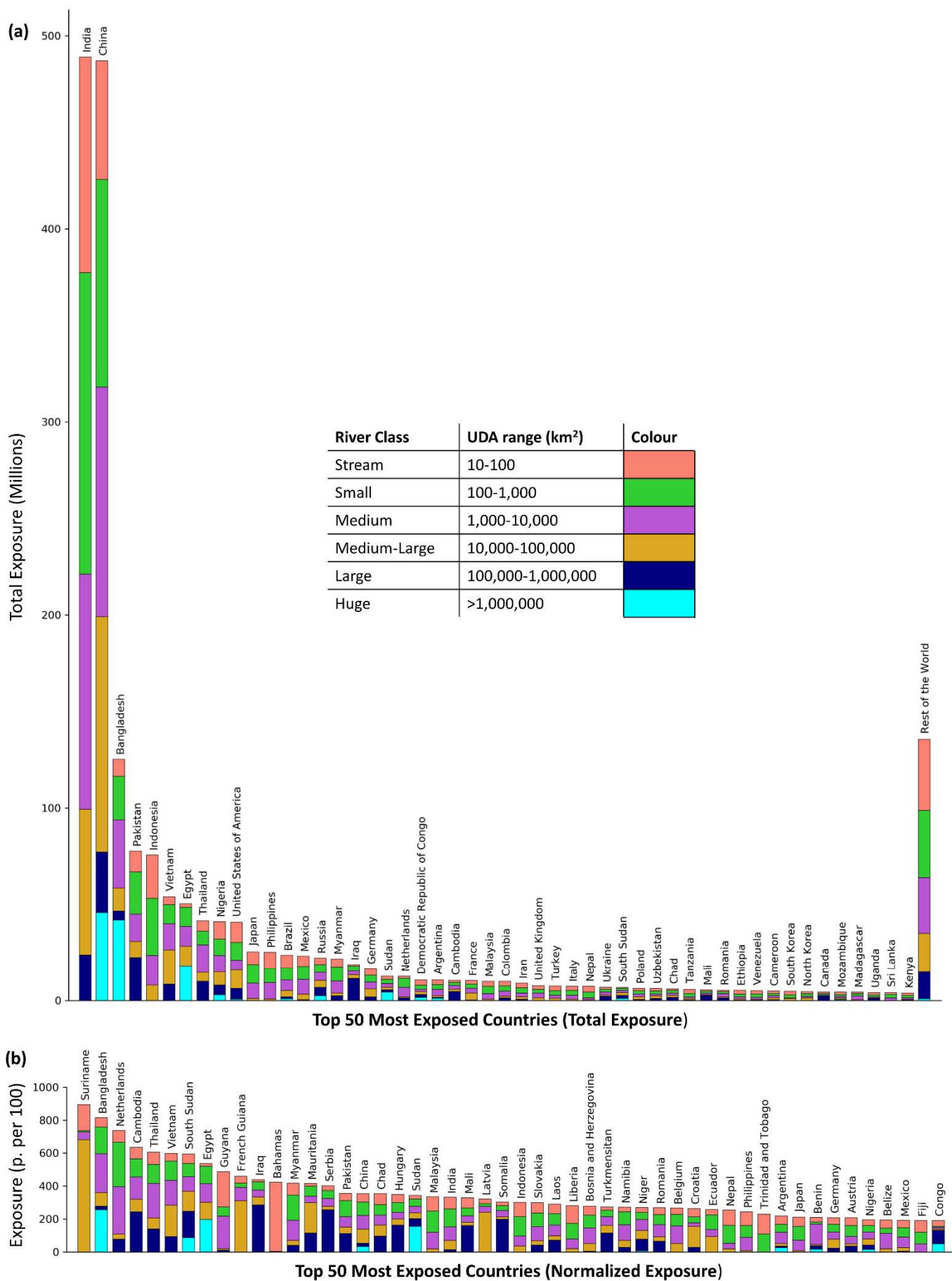


Figure S14. WorldPop calculated flood exposure. (a) Top 50 most exposed countries in terms of total flood exposure. (b) Top 50 most exposed countries in terms of normalized flood exposure (normalized to country's total population)

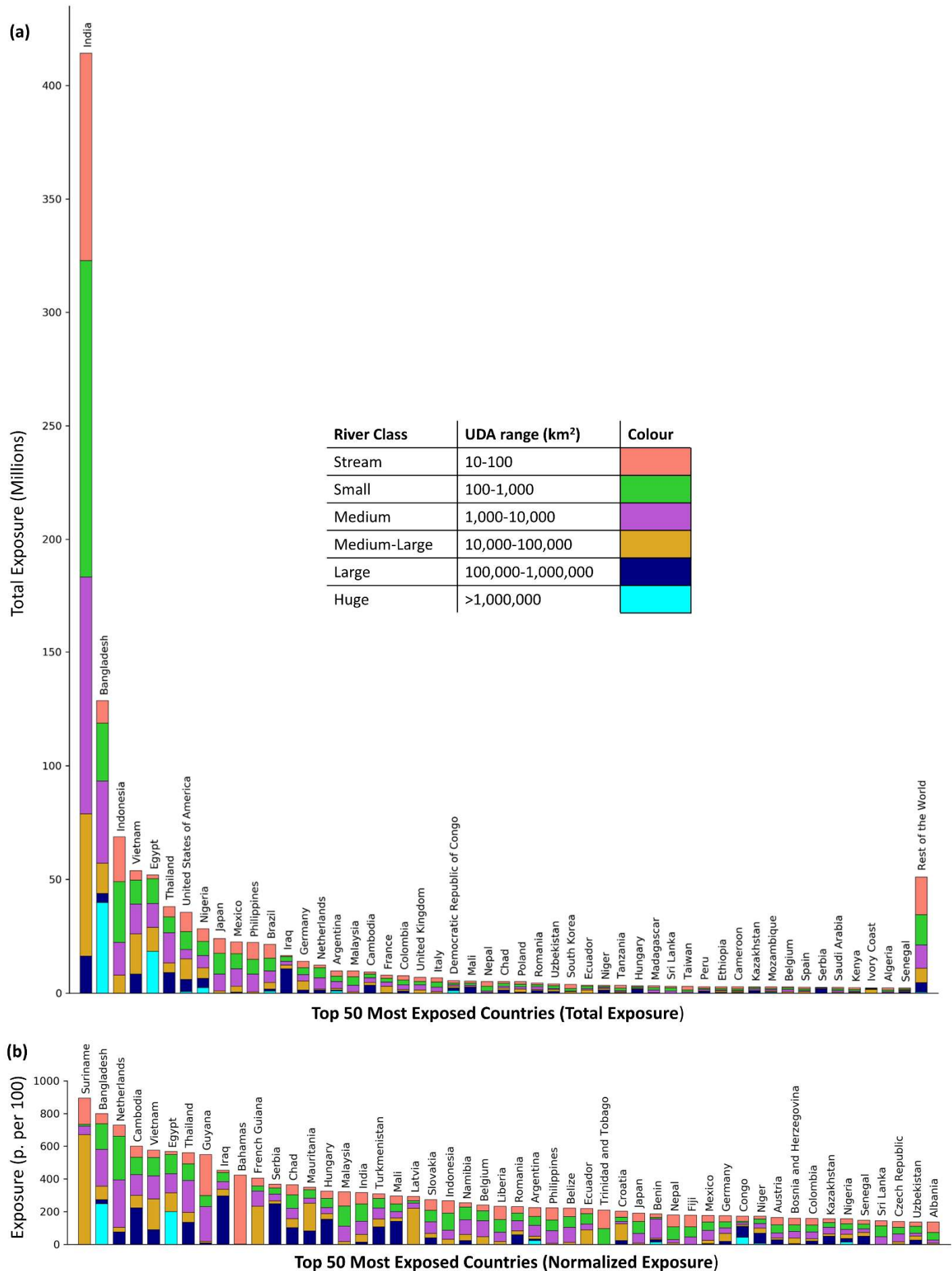


Figure S15. HRSL calculated flood exposure. (a) Top 50 most exposed countries in terms of total flood exposure. (b) Top 50 most exposed countries in terms of normalized flood exposure (normalized to country's total population). Note: flood exposure is calculated only for the 168 countries where HRSL is available. For countries missing from this analysis see Table S7.

S4 HRSL Missing Countries

Table S10. Countries not mapped by HRSL (at time of writing). These countries were not represented in any of the results calculated using the HRSL dataset.

Aaland Islands	Gibraltar	Pakistan
Afghanistan	Guernsey	Palestine
Antarctica	Iran	Russia
Andorra	Isle of Man	Saint Pierre and Miquelon
Armenia	Israel	Saint-Barthelemy
Azerbaijan	Jersey	Saint-Martin (French)
Bhutan	Kosovo	Sint Maarten (Dutch)
Brunei	Kuwait	Somalia
Canada	Laos	South Sudan
China	Lebanon	Sudan
Cuba	Luxembourg	Sweden
Curacao	Martinique	Sweden
Cyprus	Montserrat	Syria
Denmark	Morocco	Turkey
Falkland Islands	Myanmar	Ukraine
Faroe Islands	Norfolk Island	Vatican City
Finland	North Korea	Venezuela
Georgia	Norway	Yemen

S5 GFM Coverage Maps

WorldPop

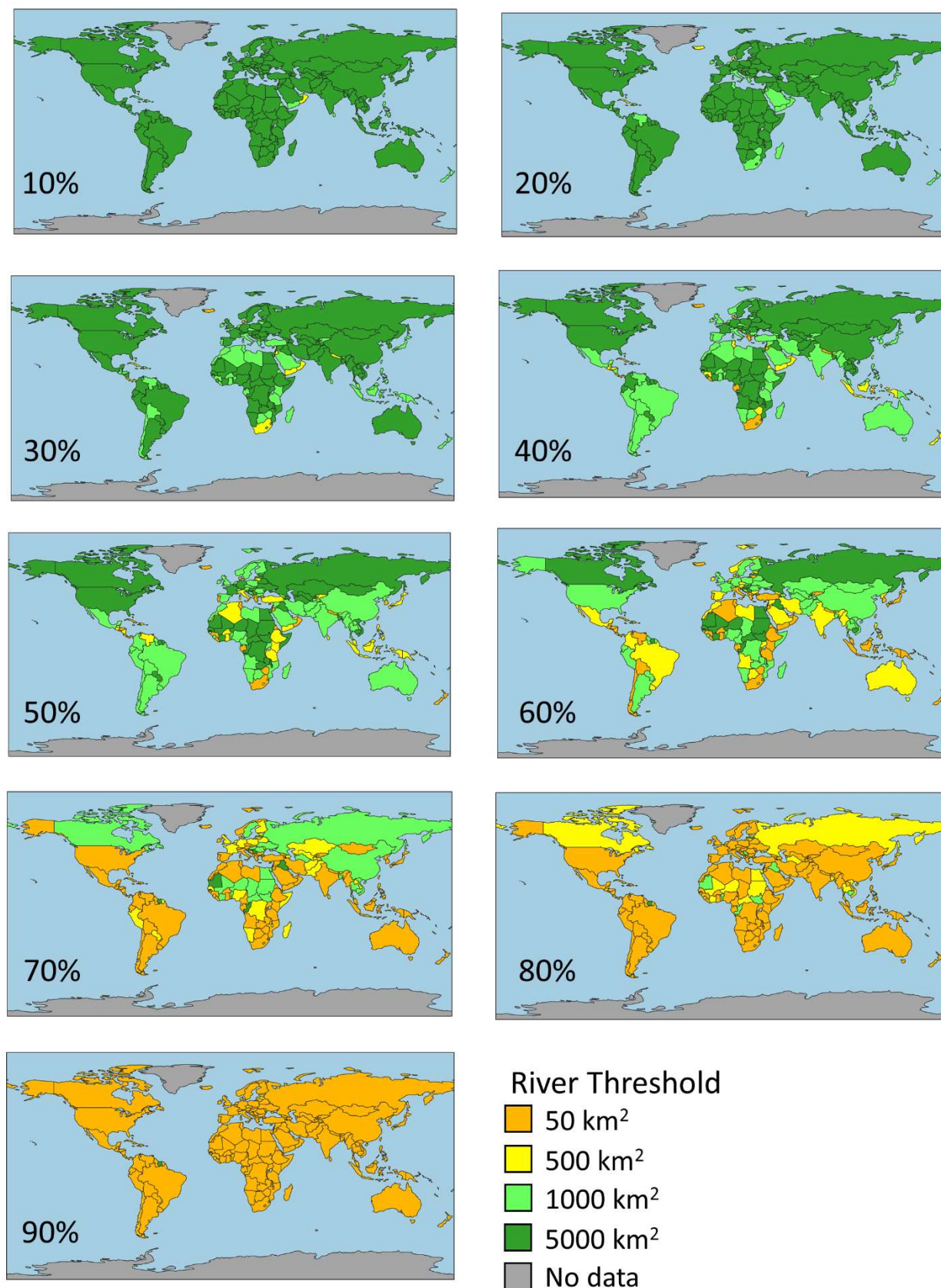


Figure S16. What size GFM river initiation threshold is required to capture _% of a country's total GFM flood (>50 km²) exposure. Each map is a different target percentage. This map is intended to inform users of GFM about the appropriate GFM to use in a given country. Results were calculated using WorldPop population data.

GHSL

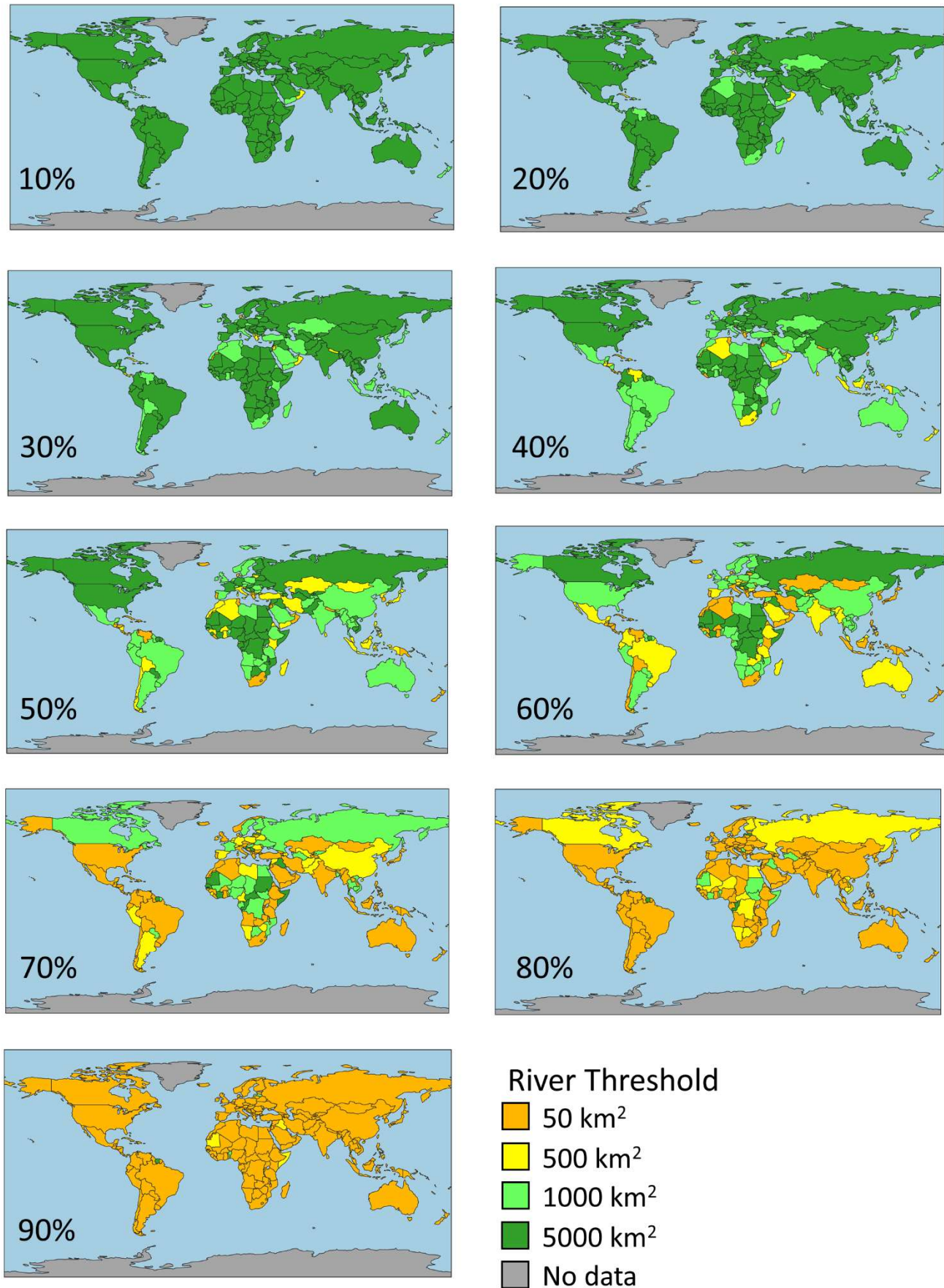


Figure S17. What size GFM river initiation threshold is required to capture _% of a country's total GFM flood (>50 km²) exposure. Each map is a different target percentage. This map is intended to inform users of GFM's about the appropriate GFM to use in a given country. Results were calculated using GHSL population data.

HRSL

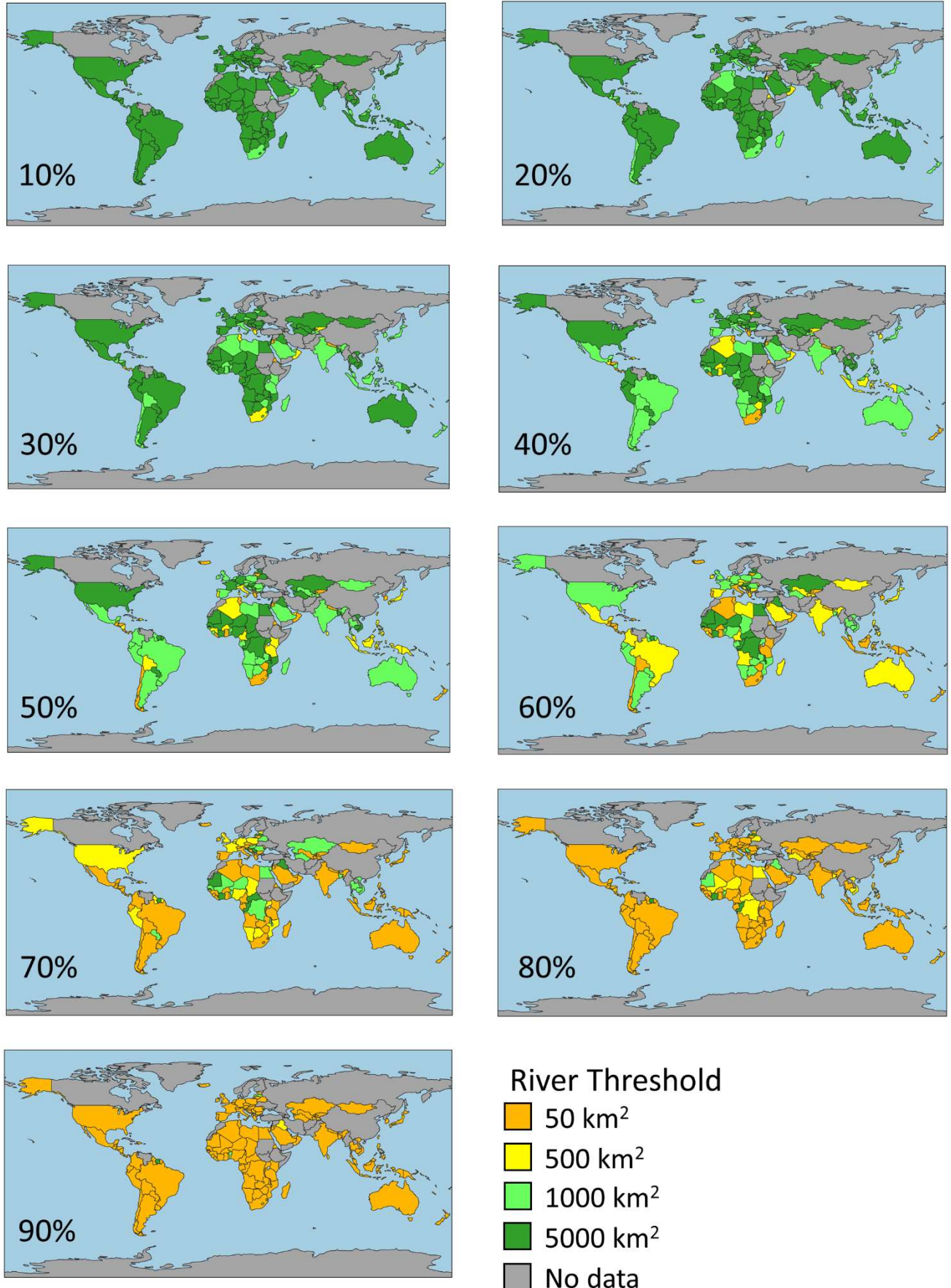


Figure S18. What size GFM river initiation threshold is required to capture _% of a country's total GFM flood (>50 km²) exposure. Each map is a different target percentage. This map is intended to inform users of GFM's about the appropriate GFM to use in a given country. Results were calculated using HRSL population data.

S6 References

- BECK, H. E., ZIMMERMANN, N. E., MCVICAR, T. R., VERGOPOLAN, N., BERG, A. & WOOD, E. F. 2018. Present and future Köppen-Geiger climate classification maps at 1-km resolution. *Scientific Data*, 5, 180214.
- BERNHOFEN, M. V., WHYMAN, C., TRIGG, M. A., SLEIGH, P. A., SMITH, A., SAMPSON, C., YAMAZAKI, D., WARD, P., RUDARI, R., PAPPENBERGER, F., DOTTORI, F., SALAMON, P. & WINSEMIUS, H. C. 2018a. Analysis inputs for validation of six global flood models against observed flood events in Nigeria and Mozambique. Research Data Leeds Repository.
- BERNHOFEN, M. V., WHYMAN, C., TRIGG, M. A., SLEIGH, P. A., SMITH, A. M., SAMPSON, C. C., YAMAZAKI, D., WARD, P. J., RUDARI, R., PAPPENBERGER, F., DOTTORI, F., SALAMON, P. & WINSEMIUS, H. C. 2018b. A first collective validation of global fluvial flood models for major floods in Nigeria and Mozambique. *Environmental Research Letters*, 13.
- DOTTORI, F., ALFIERI, L., SALAMON, P., BIANCHI, A., FEYEN, L. & HIRPA, F. A. 2016a. Flood hazard map of the World - 100-year return period. In: EUROPEAN COMMISSION, J. R. C. J. (ed.).
- DOTTORI, F., ALFIERI, L., SALAMON, P., BIANCHI, A., FEYEN, L. & LORINI, V. 2016b. Flood hazard map for Europe, 100-year return period. In: EUROPEAN COMMISSION, J. R. C. J. (ed.).
- DOTTORI, F., SALAMON, P., BIANCHI, A., ALFIERI, L., HIRPA, F. A. & FEYEN, L. 2016c. Development and evaluation of a framework for global flood hazard mapping. *Advances in Water Resources*, 94, 87-102.
- LEHNER, B. & GRILL, G. 2013. Global river hydrography and network routing: baseline data and new approaches to study the world's large river systems. *Hydrological Processes*.
- NARDI, F., ANNIS, A., DI BALDASSARRE, G., VIVONI, E. R. & GRIMALDI, S. 2019. GFPLAIN250m, a global high-resolution dataset of Earth's floodplains. *Scientific Data*, 6, 180309.
- PAPPENBERGER, F., DUTRA, E., WETTERHALL, F. & CLOKE, H. L. 2012. Deriving global flood hazard maps of fluvial floods through a physical model cascade. *Hydrology and Earth System Sciences*, 16, 4143-4156.
- RUDARI, R., SILVESTRO, F., CAMPO, L., REBORA, N., BONI, G. & HEROLD, C. 2015. IMPROVEMENT OF THE GLOBAL FLOOD MODEL FOR THE GAR 2015.
- SAMPSON, C. C., SMITH, A. M., BATES, P. B., NEAL, J. C., ALFIERI, L. & FREER, J. E. 2015. A high-resolution global flood hazard model. *Water Resources Research*, 51, 7358-7381.
- TRIGG, M. A., BIRCH, C. E., NEAL, J., BATES, P., SMITH, A., SAMPSON, C., YAMAZAKI, D., HIRABAYASHI, Y., PAPPENBERGER, F., DUTRA, E., WARD, P. J., WINSEMIUS, H. C., SALAMON, P., DOTTORI, F., RUDARI, R., KAPPES, M. S., SIMPSON, A., HADZILACOS, G. & FEWTRELL, T. 2016a. Aggregated fluvial flood hazard output for six Global Flood Models for the African Continent. Research Data Leeds Repository.
- TRIGG, M. A., BIRCH, C. E., NEAL, J. C., BATES, P. D., SMITH, A., SAMPSON, C. C., YAMAZAKI, D., HIRABAYASHI, Y., PAPPENBERGER, F., DUTRA, E., WARD, P. J., WINSEMIUS, H. C., SALAMON, P., DOTTORI, F., RUDARI, R., KAPPES, M. S., SIMPSON, A. L., HADZILACOS, G. & FEWTRELL, T. J. 2016b. The credibility challenge for global fluvial flood risk analysis. *Environmental Research Letters*, 11, 10.
- WINSEMIUS, H. C., VAN BEEK, L. P. H., JONGMAN, B., WARD, P. J. & BOUWMAN, A. 2013. A framework for global river flood risk assessments. *Hydrology and Earth System Sciences*, 17, 1871-1892.